Journal of the European Ceramic Society 22 (2002) 411–414

www.elsevier.com/locate/jeurceramsoc

Formation of porous alumina with oriented pores

Xiang-jin Ding*, Ji-zhou Zhang, Ruo-ding Wang, Chu-de Feng

The Research and Development Center of Functional Ceramics, Shanghai Institute of Ceramics, Chinese Academy of Sciences, Shanghai 200050, PR China

Received 14 December 2000; received in revised form 26 March 2001; accepted 28 April 2001

Abstract

Adopting the theories describing the bubble forming in the metal–hydrogen solidification process, porous alumina with oriented pores was prepared by combining a foaming method with sol-gel technology. The bubble forming process in the sol-gel is different from that in the metal–hydrogen system. Samples were calcined at temperature from 800 to 1200C. The volume-shrinkage and compressive-strength increased with increasing calcination temperature. The porous alumina exhibited a bimodal pore structure when prepared below 1200°C. © 2002 Elsevier Science Ltd. All rights reserved.

Keywords: Al; Al_2O_3; Foams; Porosity; Sol-gel processes

1. Introduction

Porous materials are widely used as molten metal and hot gas filters, as membranes for chemical processes, as thermal insulation, as catalyst supports, and as chemical sensors.[1,2] There are several ways of producing porous ceramics.[3] The foaming method is one of the most common methods to prepare porous ceramics with closed voids. It is, however, difficult to produce porous ceramics with uniform and oriented pores. Oriented gas–solid porous metals are easily formed via solidification in metal–hydrogen system.[4] In this paper, we tried to adopt the bubble formation theories from that system to prepare oriented porous alumina by sol-gel technology.

2. Theory background[4]

When a gas bubble capable of growth nucleates on the interface between a liquid and a solid, the cavity size must be greater than or equal to a certain critical radius r, which can be estimated by assuming that the surface energy of a bubble is equal to its bulk energy,

$$p\mathrm{d}V = \sigma\mathrm{d}S \tag{1}$$

where $p = p_{\mathrm{cap}} + p_{\mathrm{hydr}} + p_{\mathrm{ch}}$ is the pressure in the bubble. p_{cap} is the capillary pressure, p_{hydro} the hydrostatic pressure, p_{ch} the gas pressure in the chamber, V the bubble volume, σ the average of the specific surface energies of the gas:liquid and the gas:soild interface, S the total area of the bubble. Assuming a spherical bubble, one gets from (1)

$$4\pi r^2\mathrm{d}rp = 8\pi r\mathrm{d}r\sigma \tag{2}$$

On rearrangement,

$$pr = 2\sigma \tag{3}$$

Hence the pressure dependency of the critical radius is,

$$r = 2\sigma/p \tag{4}$$

Taking into account that the bubble is not spherical and that the specific surface energies are different, we obtain,

$$r = (\sigma_{\mathrm{GL}}K_L + \sigma_{\mathrm{GS}}K_{\mathrm{S}})/K_vP \tag{5}$$

Where σ_{GL} is the surface energy at the gas:liquid interface, σ_{GS} is the surface energy at the gas:solid interface, K_{L} and K_{S} are the coefficients accounting for the relative areas of the gas:liquid and the gas:solid

* Corresponding author.
E-mail address: tin72@yeah.net (X.-j. Ding).

PII: S0955-2219(01)00318-1

interface, K_v is the proportionality factor used in the equation for the volume of a non-spherical bubble, $V = K_v r^3$. In fact, in our experiment, the bubble formed only in the alumina sol-gel medium and did not contact the solid phase except the interface between the sol-gel and the mixture, so that the second term in the right parentheses of Eq. (5) should be omitted. Eq. (5) is rewritten as,

$$r = \sigma_{GL} K_L / K_v p \tag{6}$$

It is seen from Eq. (6) that the bubble radius r is proportional to the surface energy at the gas:liquid interface σ_{GL} and inversely proportional to the gas pressure p in the bubble.

In the liquid, a buoyancy force $F_A = (4/3)\pi r^3 \rho$ (ρ is the liquid density) will act on any bubble, inducing it to rise in the liquid. According to the Stoke's law, the velocity of the bubble's upward motion is

$$v = 2r^2 \rho / 9\eta \tag{7}$$

where η is the viscosity of the liquid. This means that the bubble growth rate is slow in a more viscous liquid, which benefits the formation of a long bubble with the possibility that it eventually become a tube.

3. Experimental

Alumina sol was prepared as reported by Yoldas.[5] The process of preparing porous alumina with oriented pores is shown in Fig. 1.

The dried alumina gel was calcined at 800, 1000 or 1200°C for 30 min, respectively. The heating rate was 0.3°C per min. SEM, XRD and BET were carried out to characterize the samples. Compressive strengths of samples were also evaluated.

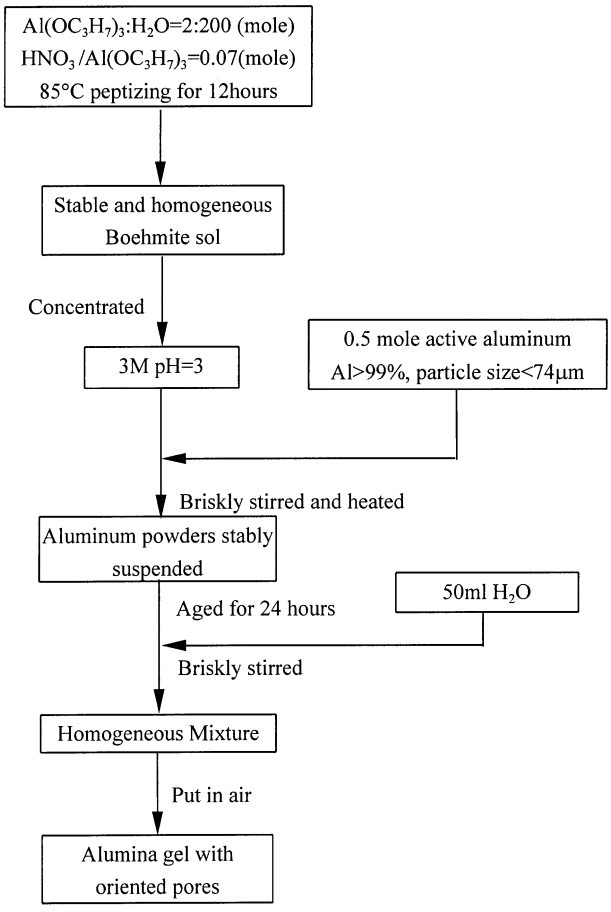

Fig. 1. The process of preparing alumina-gel with orientated pores.

4. Results and discussion

4.1. Formation of the oriented pore

Fig. 2 is a schematic diagram of bubble formation in the alumina sol-gel system. The hydrogen was released according to the reaction of pure Al with H^+ in the mixture layer:

$$Al + 3H^+ = Al^3 + 3/2H_2 \tag{8}$$

Thus, the gas pressure p in a bubble is determined by:

$$p = k^{2/3} p_0 [Al^{3+}]^{-2/3} [H^+]^2 \tag{9}$$

where k is the reaction constant, p_0 is the atmosphere pressure. This means that the p is related to the pH in

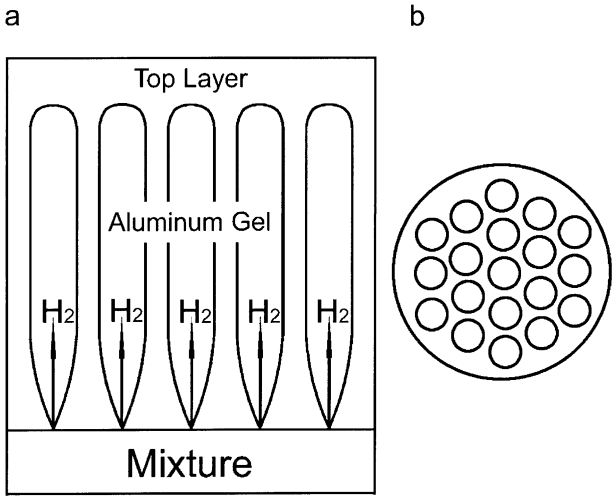

Fig. 2. Schematic diagram of the bubble formation in alumina-sol.

the alumina sol. In our experiments, the pH of the alumina sol was 3, the p is considered to be a constant. According to Eq. (6), the bubble size is determined by the p and the surface energy σ_{GL}, therefore, the lager σ_{GL} the larger bubble size. Once the bubble is formed, it would move upward by the buoyancy force according

to Eq. (7). If the concentration and pH of a sol are suitable, the gas release rate in a bubble would equate to the bubble rising velocity v caused by the buoyancy, and a long tube will appear in the sol. Fig. 3 shows the cut dried alumina gel with oriented pores. The pore diameter is about 2 mm, which might be determined by the higher σ_{GL} between the alumina sol and the hydrogen. The pore coordination number in the plane normal to the tube is typically about 6. It is very similar to that observed in the metal–hydrogen system.[4] Over the long tube, there is a thick top layer. This is attributed to the concentration gradient of the alumina sol, which is caused by the evaporation of moisture to the air.

Although the bubble formation in the alumina sol can be described by Eqs. (1)–(7), the formation of these long tubes is different from that in the metal–hydrogen. In the metal–hydrogen system, the long tube formation arises from nucleation and growth in a eutectic reaction when the metal–hydrogen system solidifies; the pore quantity and distribution pattern in the plane normal to the tube is mainly dependent on the pressure p and the presence of nucleation sites.[4] However, in the alumina-sol-aluminum system, the bubble nucleation site is mainly determined by the corrosion pattern of the aluminum.

When aluminum or aluminum alloys suffer corrosion, they do so by multiple pitting rather than by general dissolution.[6,7] The pit may start at an inclusion, a grain boundary, or some other imperfection on the metal surface, such as a dislocation; from then on, it is usually not affected by the structure of the metal. When aluminum corrodes at temperatures below 90°C in an aqueous system, the attack is usually by pitting.[7] Once pits are nucleated, their growth can be autocatalytic. Coordination of Al^{3+} with HO shifts the pH to the acidic side. Once the pH is less than about 4, the base of the pit becomes active.[6] In our experiments, the pH of the sol is about 3.0; thus, at room temperature, pitting takes place on the surface of the aluminum particle and releases hydrogen, which provides the nucleation sites for the bubble formation in the alumina sol. And the powdered aluminum benefits the homogeneity of the nucleation site distribution, which controls the quantity of the tubular bubble.[4] Fig. 4 shows SEM photographs of an aluminum particle in alumina gel and its partial magnification. The residual pit structure of the aluminum surface formed during the reaction is clearly seen in Fig. 4b. Fig. 5 shows XRD patterns of aluminum before and after reaction. There is a little bayerite on the aluminum surface before the reaction (Fig. 5a); however, more bayerite appear on the surface after reaction (Fig. 5b). It is consistent with the previous results that Al^{3+} combines with OH in the pitting process when the aluminum contacts with water.

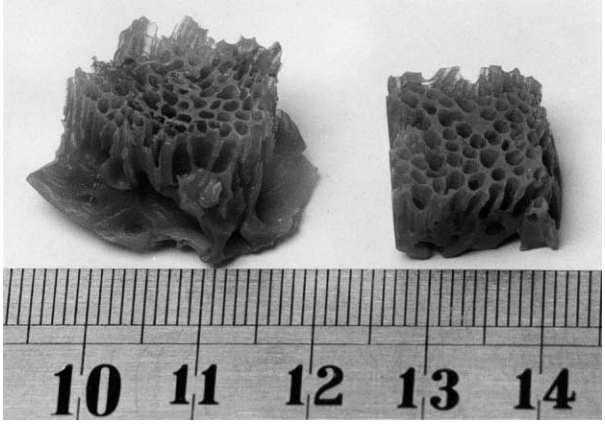

Fig. 3. Optical photograph of dried porous alumina-gel.

4.2. Characteristics of sample

Table 1 represents the characteristics of samples calcined at different temperatures. The volume shrinkage of the alumina gel after drying in air was about 90%. This high volume shrinkage easily caused stress, which resulted in cracks as seen in Fig. 6. These might be avoided by adopting other drying methods, such as supercritical drying or freeze-drying. The volume shrinkage of the sample calcined at 800°C is 20%, similar to that (21%) of the sample calcined at 1000°C. But when calcination

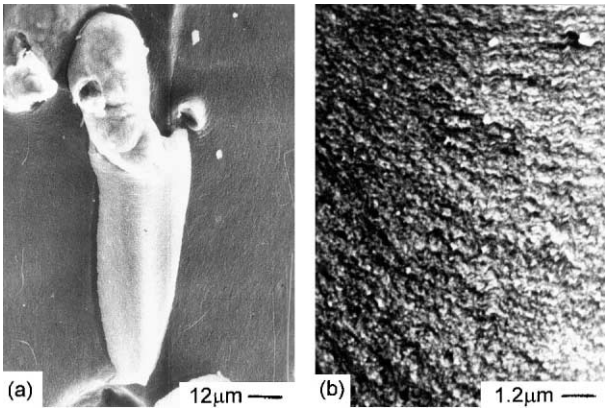

Fig. 4. Aluminum particle in alumina-gel: (a) aluminum particle; (b) surface of the aluminum particle.

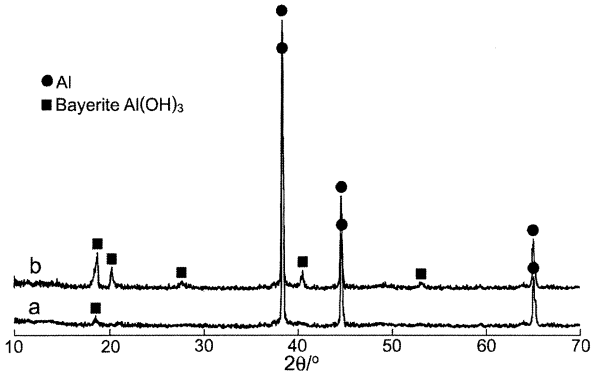

Fig. 5. XRD patterns of aluminum particle: (a) before reaction; (b) after reaction.

Table 1
Characteristics of samples calcined at different temperatures

Calcination temprature (°C)	Volume shrinkage (%)	Compressive strength (Mpa)	Mean pore diameter (mm)	Porosity of tiny pore in tube wall cm^3/g
800	20	1.1	1.2	0.34
1000	21	1.5	1.2	0.30
1200	44	2.9	1.1	0.014

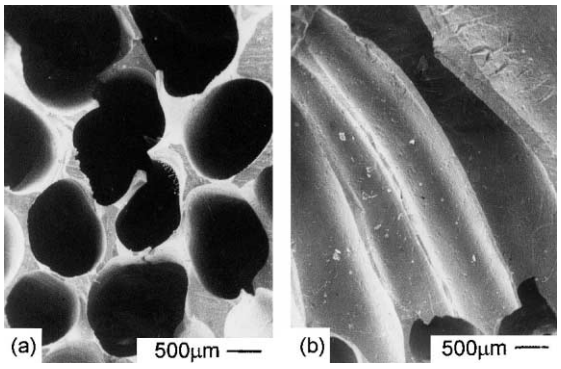

Fig. 6. SEM photograph of dried alumina-gel: (a) cross-section; (b) longitudinal section.

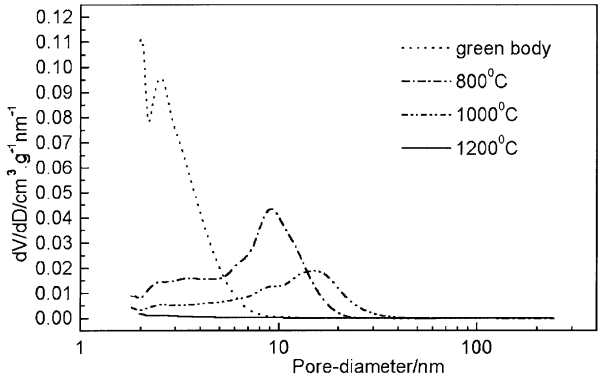

Fig. 7. Pore-size distribution of the tiny pore in the tube wall.

temperature is at 1200°C, the volume shrinkage of sample abruptly increases to 44%. These results are consistent with the transformation of boehmite to α-alumina.[8] In the range 300–500°C, boehmite gel converts to γ-alumina with modest shrinkage, but from 500 to 1000°C there is a little shrinkage. Above 1000°C, shrinkage increases rapidly until 1200°C because the γ-alumina converts to α-alumina, which causes the substantial volume shrinkage.

The compressive-strength increases with calcination temperature increasing as shown in Table 1. At 1200°C, boehmite completely converts to α-alumina, the densificaiton process within the pore wall provides the compressive-strength increase.

The porous alumina possesses a bimodal pore structure, with large scale oriented pores and micropores in the tube walls. The mean diameter of the tube is about 1.1 mm after calcination at 1200°C. The variation of the diameter is not large with the change of the calcination temperature. But, the micropores in the pore wall is strongly dependent on the calcination temperature, their distributions at different calcination temperatures are shown in Fig. 7. In the green body, the main pore size is about 3 nm and the overall porosity is the highest. With increasing calcination temperature, the main pore size shifts to lager values with the porosity decreases. When the calcining temperature is at 1200°C, the fine porosity becomes zero.

5. Conclusions

Porous alumina with oriented pores was prepared by reaction of aluminum with H^+ using sol-gel technology. The homogeneity of the oriented pore distribution is determined by the pitting on the surface of the aluminum in the reaction of aluminum with H^+. In the process of forming oriented pores, there is a top layer built up over the oriented pores; therefore, this method might be used to prepare self-supported membranes. The volume-shrinkage and compressive-strength of porous alumina with oriented pores increased with increasing calcination temperature. The porous alumina possesses a bimodal pore structure, with large oriented pores and tiny pores in the tube wall. Above 1200°C, the fine pores disappear.

References

1. Anon, Porous materials: expanding applications. *Am. Ceram. Soc. Bull.*, 1996, **71**, 1770–1776.
2. Schaefer, D. W., Engineered porous materials. *MRS Bull.,* 1994, **19**(4), 14.
3. Saggio-Woyansky, J. and Scott, C.E., Processing of Porous Ceramics. *Am. Ceram. Soc. Bull.,* 1992, **71**, 1674–1682.
4. Shapovalov, V. I., Formation of ordered gas-solid structures via solidification in metal–hydrogen system. In *Porous and Cellular Materials for Structural Applications*, ed. D. S. Schwartz, D. S. Shih, A. G. Evans and H. N. G. Wadley. Materials Research Society, Pennsylvania, 1998, pp. 281–290.
5. Yoldas, B. E., Alumina gels that form porous transparent Al_2O_3. *J. Mater. Sci.,* 1975, **10**, 1856–1860.
6. Talbot, D. and Talbot, J., *Corrosion Science and Technology*. CRC, Washington, 1997 pp. 302.
7. Shreir, L. L., *Corrosion Vol. 1. Corrosion of Metals and Alloys*. George Newnes, London, 1963, pp. 4–23.
8. Badkar, P. A., Bailey, J. E. and Barker, H. A., Sintering behavior of boehmite sol. In *Sintering Related Phenomena*, ed. G. C. Kuczynski. Plenum, New York, 1973, pp. 311–321.